

k –Dependent Dark Matter

Parisa Arabameri¹, Zahra Davari² and Nima Khosravi¹

¹*Department of Physics, Shahid Beheshti University, 1983969411, Tehran, Iran;*

²*School of Physics, Institute for Research in Fundamental Sciences (IPM), P.O. Box 19395-5531, Tehran, Iran*

July 18, 2023

ABSTRACT

With the emersion of precise cosmology and the emergence of cosmic tensions, we are faced with the question of whether the simple model of cold dark matter needs to be extended and whether doing so can alleviate the tensions and improve our understanding of the properties of dark matter. In this study, we investigate one of the generalized models of dark matter so that the behavior of this dark matter changes according to the scale of k . In large scales (small k 's), the dark matter is cold, while it becomes warm for small scales (large k 's). This behavior is modeled phenomenologically for two different scenarios. We show that the S_8 tension can be alleviated, but the H_0 tension becomes milder while not too much.

Key words: Cold Dark Matter, Warm Dark Matter

1 INTRODUCTION

The cold dark matter (CDM) paradigm is an important feature in particle physics and cosmology, assuming cold and collisionless dark matter particles interact only gravitationally. This component is one of the main bases in the standard Λ CDM model and it is responsible for about 26% of the energy density of Universe (Scott 2020; Scolnic et al. 2018). A wide range of cosmological observations from many different epochs and at large and small scales, including CMB missions, BAO data, observations of galaxy clusters, and weak lensing experiments, supported this paradigm. However, the physical nature of DM particles remains unclear and a mystery after decades of research.

On the other hand, the CDM paradigm is remarkably successful in many aspects, especially in explaining the observed properties of large-scale structures (LSS) in the Universe (in the range ~ 1 Gpc down to ~ 10 Mpc); however, it conflicts with observations on galactic and sub-galactic scales (≤ 1 Mpc). For instance, we can point to:

- The "missing satellites problem," which refers to the fact that there is an overestimation of dwarf galaxies by the CDM model than observed in the Universe (Rubin & Ford 1970; Rubin et al. 1980; Moore et al. 1999).
- The "cusp-core problem," which refers to the fact that the CDM model predicts that dark matter halos should have a cuspy density profile at their centers, while observations suggest that they have a more constant density profile (Gentile et al. 2004).
- The "too big to fail problem," which refers to the lack of observation of the most massive halos, which are predicted to be luminous (Purcell & Zentner 2012).

The small scale crisis motivated the study of scenarios that predict damped matter fluctuations below a characteristic free-streaming scale through either modification of the primordial power spectrum or non-cold dark matter models, which modify (suppress) the power spectrum at late times. Furthermore, the recent high-precision cosmological data has shown a statistically significant discrepancy in the estimation of the current values of the Hubble parameter (H_0) and the fluctuations amplitude of density perturbations at $8 h^{-1}$ Mpc scale (σ_8) between early-time and late-time observations, which poses another challenge to the standard Λ CDM model. Early universe measurements like CMB Planck collaboration (Aghanim et al. 2020) estimate $H_0 \sim (67.0 - 68.5)$ km/s/Mpc, while late-time distance ladder measurements like SH0ES and HOLICOW collaborations report $H_0 = (74.03 \pm 1.42)$ (Riess et al. 2019).

The mentioned problems, together with the lack of understanding of the nature, mass, and dynamics of dark matter particles, have sparked several extensions and alternatives to standard dark matter models of particle physics, which are theoretically well-motivated and inspire new search strategies. There are many approaches in order to investigate dark matter, such as warm dark matter (WDM), cannibal Dark Matter (Buen-Abad et al. 2018), decaying dark matter (Davari & Khosravi 2022), dynamical dark matter, fuzzy dark matter and interacting dark matter (Loeb & Weiner 2011; Archidiacono et al. 2019).

If dark matter particles decouple from the primordial plasma when still relativistic and soon become non-relativistic, the particles are called "warm dark matter". These WDM particles would have a smaller free-streaming length than cold dark matter particles, preventing them from clustering on small scales and potentially solving the missing satellite prob-

lem. Furthermore, the WDM particles significantly affect the clustering of matter on large k limit and could flat the inner regions of most galaxies more than the CDM model, reconciling these values with observation and alleviating the core-cusp problem. At the large k limit, DM behaves as WDM as it slightly reduces the DM preferred mass range to a size that includes a moderate initial velocity dispersion and free streaming, sufficient to erase some small scale structures. The suppression in WDM models has a variety of observable implications: abundances of galaxies at high redshift (Pacucci et al. 2013; Menci et al. 2016), high-redshift gamma-ray bursts (GRBs) (de Souza et al. 2013), strong gravitational lensing (Gilman et al. 2020; Hsueh et al. 2020). One extension of WDM is to assume that DM comes in two components, a cold one and a warm one, which can be produced via two co-existing mechanisms. These models are called mixed dark matter (MDM) (Maccio et al. 2013; Diamanti et al. 2017; Paribelli et al. 2021).

In this paper, we decided to investigate the case that dark matter consists of only one component, but its behavior depends on k -scale such that in small k it behaves like cold DM, and in large k it shows the properties of warm DM. This scale dependent transition in the behavior can have some motivations in the physics of critical phenomena. The k -Dependent dark energy has been studied in Farhang & Khosravi (2023) based on a phenomenological gravitational phase transition model (Khosravi & Farhang 2022; Farhang & Khosravi 2021).

The outline of this paper is as follows: in section 2, we derive Boltzmann equations governing the evolution at the perturbation level. Then, we implement the related equations in the publicly available numerical code CLASS¹ (the Cosmic Linear Anisotropy Solving System) (Lesgourgues & Tram 2011) and using the code MONTEPYTHON-v3² (Audren et al. 2013; Brinckmann & Lesgourgues 2019) to perform a Monte Carlo Markov chain (MCMC) analysis with a Metropolis-Hasting algorithm against the high- CMB TT, TE, EE +low- TT, EE+lensing data from Planck 2018 (Aghanim et al. 2020) in combination with other probes such as the Baryon acoustic oscillations, BAO (BOSS DR12 (Alam et al. 2017), eBOSS Ly- α combined correlations).

2 PHENOMENOLOGY OF k -DEPENDENT DM MODEL IN PERTURBATION LEVEL

In the framework of general relativity, let us consider the flat, homogeneous, and isotropic universe with energy density $\rho(\tau)$ and pressure $P(\tau)$ that is described by the FLRW metric. Using the Einstein equations, we can obtain the following evolution equations for the expansion factor $a(\tau)$.

$$\left(\frac{\dot{a}}{a}\right)^2 = \frac{8\pi G}{3}a^2\rho, \quad (1)$$

$$\frac{d}{d\tau}\left(\frac{\dot{a}}{a}\right) = -\frac{4\pi G}{3}a^2(\rho + 3P), \quad (2)$$

where the dots denote derivatives with respect to conformal time, τ . The most convenient way to solve the linearized Einstein equations is in the two gauges in the Fourier space k . In

the synchronous gauge, the scalar perturbations are characterized by $h(\vec{k}, \tau)$ and $\eta(\vec{k}, \tau)$. The scalar mode of h_{ij} is given as a Fourier integral

$$h_{ij}(\vec{x}, \tau) = \int d^3k \left(h(\vec{k}, \tau) \hat{k}_i \hat{k}_j + 6\eta(\vec{k}, \tau) \left(\hat{k}_i \hat{k}_j - \frac{1}{3} \delta_{ij} \right) \right) e^{i\vec{k}\cdot\vec{x}}, \quad (3)$$

where, h is used to denote the trace of h_{ij} in both the real space and the Fourier space (Aoyama et al. 2014).

The perturbations are characterized by two scalar potentials $\psi(\tau, \vec{x})$ and $\phi(\tau, \vec{x})$ which appear in the line element as

$$ds^2 = a^2(\tau) \left(-(1 + 2\psi)d\tau^2 + (1 - 2\phi)d\vec{x}^2 \right), \quad (4)$$

and for a perfect fluid of energy density, ρ , and pressure, P , the energy-momentum tensor has the form

$$T_\nu^\mu = P g_\nu^\mu + (\rho + P)u^\mu u_\nu, \quad (5)$$

where u^μ is the four-velocity of the fluid. The perturbed part of energy-momentum conservation equations in k -space implies the synchronous gauge as

$$\dot{\delta} = -3\mathcal{H}(c_s^2 - w)\delta - (1 + w)(\theta + \frac{\dot{h}}{2}), \quad (6)$$

$$\dot{\theta} = -\mathcal{H}(1 - 3c_g^2)\theta + \frac{c_s^2}{1 + w}k^2\delta - k^2\sigma, \quad (7)$$

and for the conformal Newtonian gauge as

$$\begin{aligned} \dot{\delta} &= -3\mathcal{H}(c_s^2 - w)\delta - (1 + w)(\theta - 3\dot{\phi}), \\ \dot{\theta} &= -\mathcal{H}(1 - 3c_g^2)\theta + \frac{c_s^2}{1 + w}k^2\delta - k^2\sigma + k^2\psi. \end{aligned} \quad (8)$$

The evolution equation for the shear can be obtained as

$$\dot{\sigma} = -3\left[\frac{1}{\tau} + \mathcal{H}\left(\frac{2}{3} - c_g^2 - \frac{1}{3}\frac{\mathcal{P}}{p}\right)\right]\sigma + \frac{4}{3}\frac{c_{\text{vis}}^2}{1 + w}(2\theta + \dot{h}). \quad (9)$$

c_s and c_g in the above equations are the effective sound speed and the adiabatic sound speed, respectively. In equation 9, c_{vis}^2 is a new parameter named viscosity speed, and in implementation of CLASS, it is assumed as $c_{\text{vis}}^2 = 3wc_g^2$ (Lesgourgues & Tram 2011). The adiabatic sound speed can be expressed as

$$c_g^2 = \frac{\dot{p}}{\dot{\rho}} = w - \frac{\dot{w}}{3\mathcal{H}(1 + w)}, \quad (10)$$

or in another form $c_g^2 = \frac{\dot{p}}{\dot{\rho}} = -w\frac{\dot{p}}{p}\left(\frac{\dot{a}}{a}\right)^{-1}\frac{1}{3(1+w)}$, that it is stated in Tram et al. (2019), $\frac{\dot{p}}{p} = \left(\frac{\dot{a}}{a}\right)\left(5 - \frac{\mathcal{P}}{p}\right)$. So, the adiabatic sound speed can be rewrote as

$$c_g^2 = \frac{w}{3(1 + w)}\left(5 - \frac{\mathcal{P}}{p}\right), \quad (11)$$

here \mathcal{P} is the pseudo-pressure that for any pressureless species, $\mathcal{P} \simeq p \simeq 0$ and for relativistic species we have $\mathcal{P} \simeq p$ since in a higher moment pressure $\frac{\mathcal{P}}{p} \simeq 1$.

Obtaining an analytical expression for c_s^2 is more complicated since there is no dynamic equation for pressure perturbation, so in Abellán et al. (2021) and Lesgourgues & Tram (2011), it is supposed that c_s^2 is scale-independent and approximately equal to c_g^2 . Nevertheless, the full Boltzmann hierarchy calculations show that c_s^2 represents a specific k -dependence and cannot be obtained with a background quantity such as c_g^2 ,

¹ https://github.com/lesgourg/class_public

² https://github.com/baudren/montepython_public

and it increases slightly on the scales k . We follow the prescription in [Abellán et al. \(2021\)](#) for the synchronous sound speed as

$$c_s^2(k) = c_g^2 \left[1 + \frac{1}{5} \sqrt{\frac{k}{k_{fs}}} \right], \quad (12)$$

where $k_{fs} = \sqrt{\frac{3}{2} \mathcal{H}(a)/c_g(a)}$ is the free-streaming length of the WDM particles.

Equations 6-9 are valid for a single uncoupled fluid or for the net (mass-averaged) δ and θ for all fluids. They need to be modified for individual components if the components interact with each other.

The CDM particles can be used to define the synchronous coordinates and therefore have zero peculiar velocities in this gauge. Setting $\theta = \sigma = 0$ and $w = \dot{w} = 0$ in equation 6 for synchronous gauge lead to

$$\dot{\delta}_{\text{CDM}} = -\frac{1}{2}\dot{h}. \quad (13)$$

However, the CDM fluid velocity in the conformal Newtonian gauge is not zero in general. In k -space, equation 8 gives

$$\dot{\delta}_{\text{CDM}} = -\theta_{\text{CDM}} + 3\dot{\phi}, \quad \dot{\theta}_{\text{CDM}} = -\frac{\dot{a}}{a}\theta_{\text{CDM}} + k^2\psi. \quad (14)$$

As we mentioned, in this study, we intend to consider dark matter such that its behavior changes in terms of scale, so it behaves as relativistic such as warm dark matter particles in large k scales, and as non-relativistic such as cold dark matter in small k scales. Therefore, we introduce a step function, $\mathcal{S}(k)$, for switching between these two boundary conditions. $\mathcal{S}(k)$ could be any kind of step (switching) function; for example we consider it as

$$\mathcal{S}(k) = \frac{1 + \tanh[\alpha(k - k_0)]}{2}. \quad (15)$$

α and k_0 are free parameters that α control the smoothness of the transition between cold and warm dark matter. We rewrite 6 by using $\mathcal{S}(k)$ as

$$\dot{\delta} = \frac{\dot{h}}{2} + \mathcal{S}(k) [-3\mathcal{H}(c_s^2 - w)\delta - (1 + w)\theta], \quad (16)$$

$$\dot{\theta} = \mathcal{S}(k) [-\mathcal{H}(1 - 3c_g^2)\theta + \frac{c_s^2}{1 + w}k^2\delta - k^2\sigma], \quad (17)$$

$$\dot{\sigma} = \mathcal{S}(k) \left[-3\left(\frac{1}{\tau} + \mathcal{H}\left(\frac{2}{3} - c_g^2 - \frac{1}{3}p\right)\right)\sigma + \frac{4}{3} \frac{c_{\text{vis}}^2}{1 + w}(2\theta + \dot{h}) \right]. \quad (18)$$

It is obvious that if $\mathcal{S}(k)$ vanishes, the above equations reduce to the CDM. This case happens for $k < k_0$ and is more precise for larger α 's.

We implement the above equations in the public Boltzmann solver CLASS. Since we expect this model to behave similarly to CDM in the cosmological background, we only change the perturbation equations in module `perturbation.c`. We analyzed this model in two cases: i) the sound speed behaves independently of k as a constant parameter (k -DM(1)) and ii) the case where it changes depending on k given to equation 12 (k -DM(2)).

3 k -DEPENDENT DM MODEL VERSE DATA

In this section, we present constraints on the k -Dependent dark matter model we have introduced. For MCMC analysis, we use the Metropolis-Hastings algorithm of the cosmological sampling package MONTEPYTHON-v3, connected to an altered version of the Boltzmann Solver CLASS.

We use the following dataset combination to perform statistical inference:

- CMB: We use the CMB temperature and polarization auto- and cross-correlation measurements of the most recent Planck 2018 legacy release, including the full temperature power spectrum at multipoles $2 \leq l \leq 2500$ and the polarization power spectra in the range $2 \leq l \leq 29$ (lowP). We also include information on the gravitational lensing power spectrum estimated from the CMB trispectrum analysis. ([Aghanim et al. 2020](#)).

- BAO: We use the BAO measurements from the Baryon Oscillation Spectroscopic Survey Data Release 12 (BOSS DR12) ([Alam et al. 2017](#)), SS DR14-Ly- α combined correlations ([de Sainte Agathe et al. 2019](#)), Lyman- α forest autocorrelation [de Sainte Agathe et al. \(2019\)](#), and the cross correlation of Lyman- α and QSO ([Blomqvist et al. 2019](#)).

- LSS: We use three different sets of LSS data in order to check whether k -Dependent dark matter model leads to a suppression in the matter power spectrum relative to the CDM:

- 1- KiDS + Viking 450 (KV450) matter power spectrum shape data; this combined analysis of data from the KiloDegree Survey (KiDS) and the VISTA Kilo-Degree Infrared Galaxy Survey (VIKING) includes photometric redshift measurements with cosmic shear/weak-lensing observations to measure the matter power spectrum over a wide range of k -scales at redshifts between 0.1 and 1.2 ([Hildebrandt et al. 2020](#)).

- 2- Planck SZ (2013): Another independent LSS dataset is the Planck SZ which studies the properties of galaxy clusters by measuring the Sunyaev-Zeldovich effect. But we should note that the measurements of galaxy distribution from the SZ effect depend on a mass bias factor $(1 - b)$ that relates the observed SZ signal to the true mass of galaxy clusters. In Planck SZ (2013), a numerical simulation of the S_8 measurement is reported by fixing the mass bias to its central value $(1 - b) = 0.8$. Later, the Planck SZ (2015) report allowed $(1 - b)$ to vary with a Gaussian prior centered at 0.79. The central value of the resulting S_8^{SZ} becomes smaller but has a much larger uncertainty, $S_8^{\text{SZ}} = 0.744 \pm 0.034$, and less tension to CMB measurements ([Ade et al. 2016](#)). For our analysis, we chose this data set since the central value σ_8 of the SZ (2013) analysis is consistent with many low-redshift measurements ([Zu et al. 2023](#)).

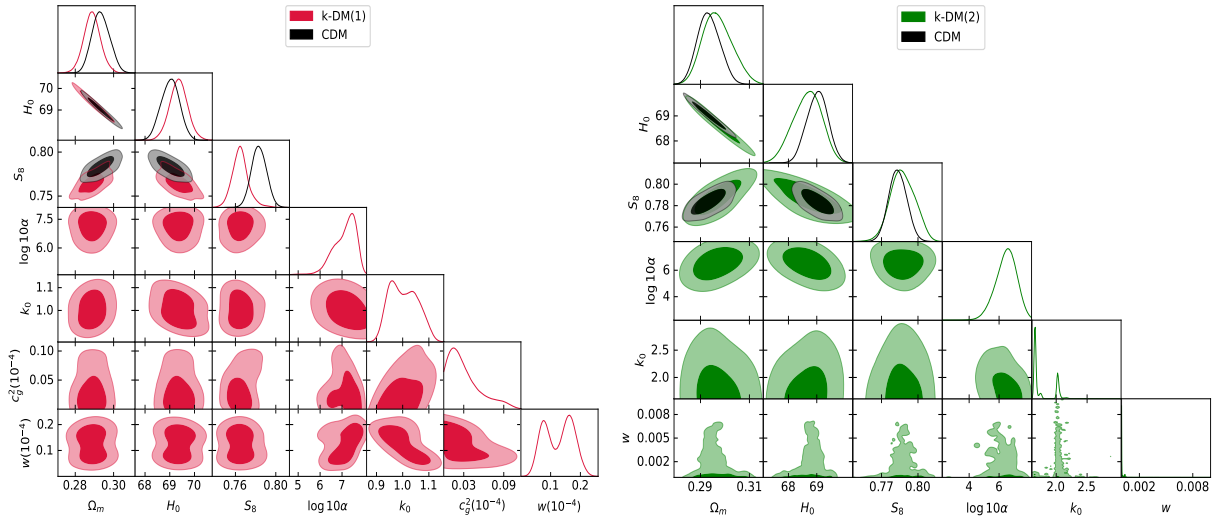
- 3-WiggleZ $P(k)$ data: Since dark energy has an effect on the expansion history of the Universe and on the growth of cosmological structures, we also use WiggleZ data in this study. The WiggleZ Dark Energy Survey is a survey to measure the large scale structure of the Universe by mapping the distance-redshift relation with baryon acoustic oscillations ([Kazin et al. 2014](#)).

We employ the χ^2 statistics to constrain our theoretical model as:

$$\chi^2 = \frac{(\mathcal{P}_{\text{obs}} - \mathcal{P}_{\text{th}})^2}{\sigma_{\mathcal{P}}^2}, \quad (19)$$

Table 1. The best and mean values and 68% confidence limit (CL) constraints for the free parameters of CDM and two k -DM models. They are given using Planck and Planck+Other datasets described in the paper.

Model	Parameter	<i>Planck</i>		<i>Planck + Other</i>	
		best-fit	$mean \pm \sigma$	best-fit	$mean \pm \sigma$
k -DM(1)	Ω_m	0.3113	0.3148 ± 0.0067	0.2903	0.2888 ± 0.0044
	$\log_{10} \alpha$	7.59	$7.88^{+0.15}_{-0.12}$	7.72	$7.14^{+0.61}_{-0.34}$
	k_0	1.68	$1.70^{+0.19}_{-0.12}$	0.988	$1.003^{+0.049}_{-0.065}$
	c_g^2	0.052	< 0.014	$0.0116(10^{-4})$	$< 0.0373(10^{-4})$
	w	0.011	< 0.009	$0.181(10^{-4})$	$0.126 \pm 0.049(10^{-4})$
	H_0	67.67	67.40 ± 0.49	69.25	69.36 ± 0.36
	S_8	0.8280	0.829 ± 0.012	0.7651	$0.7649^{+0.0067}_{-0.0083}$
k -DM(2)	Ω_m	0.3107	0.3129 ± 0.0073	0.2954	$0.2969^{+0.0054}_{-0.0066}$
	$\log_{10} \alpha$	7.65	$7.7^{+1.4}_{-1.1}$	6.54	$6.49^{+0.77}_{-0.63}$
	k_0	2.51	12^{+15}_{-10}	1.66	$1.93^{+0.11}_{-0.30}$
	w	0.570	< 0.532	$1.18(10^{-7})$	$< 5.48(10^{-5})$
	H_0	67.66	67.54 ± 0.53	68.84	$68.67^{+0.55}_{-0.48}$
	S_8	0.822	0.826 ± 0.013	0.7795	0.7875 ± 0.0099
CDM	Ω_m	0.313328	0.3142 ± 0.0065	0.2929	0.2933 ± 0.0045
	H_0	67.52	67.46 ± 0.47	69.47	69.02 ± 0.37
	S_8	0.828789	0.831 ± 0.0012	0.7872	0.7833 ± 0.0074

**Figure 1.** 1D likelihoods and 2D contours in 68% and 95% CL marginalized joint regions for chosen free parameters while they are constrained by using *Planck + Other* datasets. It seems the k -DM models predict lower S_8 to alleviate this tension while the H_0 value is not affected too much.

here \mathcal{P}_{obs} , \mathcal{P}_{th} and $\sigma_{\mathcal{P}}^2$ indicate the observed values, the predicted values and the standard deviation, respectively. Note that in addition to the six free parameters of the standard model, i.e. $(\Omega_b, \Omega_{DM}, 10\theta_{MC}, \ln 10^{10} A_s, n_s, \tau_{\text{reio}})$, the k -Dependent dark matter model introduced in the previous section includes for the first case: (α, k_0, w, c_g^2) and the second case: (α, k_0, w) . To span the α parameter's space, we work

with $\log_{10} \alpha$ instead of α . The flat priors we assumed for the parameters are given by $k_0 \in [0, 10]$, $\alpha \in [0, 10^{10}]$, $w \in [0, 1]$, and $c_g^2 \in [0, 1]$. The convergence of chains for each parameter is measured by the Gelman-Rubin criterion, and one can obtain acceptable $R - 1$ values (i.e., below 0.01 for every parameter) with an iterative strategy (Gelman & Rubin 1992) and the average acceptance rate (acc) is around 0.2.

In order to check the cosmic tensions in these models, we added data step by step in two MCMC scans as: Planck and then Planck+Other. This can provide us with further intuition as a starting point, given that Planck’s data has provided the most precise measurements of the early universe.

In the Table 1, we report the best and the mean values and 68% CL intervals for the main parameters, including the total matter density parameter ($\Omega_m = \Omega_B + \Omega_{DM}$), the present-day expansion rate of the Universe or the Hubble constant, H_0 , and $S_8 = \sigma_8 \sqrt{\Omega_m/0.3}$ in different scenarios for two MCMC analyzes. We also show posterior distributions (1σ and 2σ intervals) as dark and light-shaded contours for MCMC analysis, respectively, in the plots of the Figure 1.

Some points in these plots need to be stressed. First, it is clear that by considering all different data sets, the parameters are bound more tightly than the analysis with Planck data³. Second, we can see that the decrease of H_0 values are associated with the increase of Ω_m values and vice versa in both k -Dependent and cold dark matter scenarios. As we see in Table 1, assuming k dependence of dark matter behavior for the Planck+Other analysis seems to improve the S_8 tension for the k -Dependent dark matter scenario. However, we do not see any significant improvement in addressing the H_0 tension. Note that the results show a small deviation from CDM due to non-zero values for w and c_g^2 when we have Planck+Other datasets. Their values are at order $\mathcal{O}(10^{-5})$, which are in agreement with generalized dark matter models (Ilić et al. 2021; Kopp et al. 2016).

Next, to check whether the fit is good and also to choose the best and most compatible model with the observational data, we employ the simplest method that is usually used in cosmology, which is called the least squares method, χ_{tot}^2 . In this case, the model with smaller χ_{tot}^2 is taken to be a better fit to the data (Davari & Rahvar 2021). Comparing k -Dependent model to the CDM scenario, we note that k -Dependent DM model does better than the CDM model. However, one can have the impression that the model with the lowest χ_{tot}^2 is not necessarily the best because adding more flexibility with extra parameters will normally lead to a lower χ_{tot}^2 . In this work, the k -Dependent model has three more parameters than the CDM scenario. In order to deal with model selection, a standard approach is to compute the Akaike Information Criterion (AIC). It is defined as

$$AIC = \chi_{min}^2 + 2M + \frac{2M(M+1)}{N-M+1}, \quad (20)$$

where M is the number of free parameters in the model and N is the number of data points; thus, $\Delta AIC = \Delta \chi_{min}^2 + 2\Delta M$. We neglect the third term in the Equation 20 for large sample sizes, $N \geq M$. We report the result of MCMC analysis for the best-fit χ_{min}^2 for observational Planck and total data sets and for both models in Table 2.

The results of this analysis can be interpreted with the Jeffreys’ scale as follows: among all models, the one that minimizes the AIC is considered to be the best one, and if the difference between the AIC of a given model and the best model

is smaller than 4, one concludes that the data equally support the best fitted model and a given model. In the case of $4 < |\Delta AIC| < 10$, observations still support the given model but less than the best one. Finally, for $|\Delta AIC| > 10$, observations basically do not support the given model compared to the best model (Davari et al. 2018). According to Table 2, the only Planck data prefers CDM with respect to k -DM models. However, adding the other datasets make the situation in favor of k -DM models. This may mean that k -DM models have more space to include all the datasets altogether. In order to have a better understanding of the aspects of obtaining from MCMC scans, in the following, we discuss the features of the k -Dependent model in the CMB and the matter power spectrum. In Figure 2, we show the matter power spectrum, $P(k) \equiv \langle \delta_m(k) \rangle^2$, in the k -Dependent model relative to the CDM model for the best obtained values using Planck+Other data. As we see, k -Dependent dark matter case mimics the CDM scenario to $k \simeq 1.3$ for the k -DM(1) and $k \simeq 2.2hMpc^{-1}$ for the k -DM(2), but then starts to deviate at larger k ’s (i.e., small scales) and suppresses the power spectrum of matter by a large difference compared to the standard model. We include the information embedded in the Ly α forest measured with the eBOSS-DR14 data release on scales of a few Mpc. One reason for this difference could be the lack of observational data in this range. In Figure 3, we notice that considering k dependence for dark matter has the influence of slowing down the evolution rate of the dark matter perturbations. This means that structures cluster slower, as we predicted from the Figure 2 for $k > 1$ with a slight difference $P_{k-DM(i)}(k) < P_{CDM}(k)$.

Since the Planck collaboration has measured the temperature and polarization maps of the CMB very precisely, it has placed stringent limits on the parameter space of the CDM model. This motivates us to study k -Dependent DM signatures in CMB maps. In Figure 4, we show how k dependency affects the temperature power spectra, including the variation with respect to the CDM model. We can see a suppression in the amplitude of the lower multipoles in the temperature power spectrum. As we know, the integrated Sachs-Wolfe (ISW) effect is important on such scales. Also, the small l ’s of CMB (TT and, even better, EE) give information on the reionization history. We obtain the redshift of the reionization, z_{reio} , using the best values of parameters to be 6.02, 6.41 and 7.38 for k -DM(1), k -DM(2) and CDM respectively. The z_{reio} of the k -DM(1) model has the biggest differences from the standard model.

A crucial quantity in determining the age and evolution of the universe in cosmology is H_0 . It represents the current rate of expansion of the universe. Because of the impact of Hubble’s expansion on the growth of matter perturbations, it is significant to survey the behavior of $H(z)$ in various DM cosmologies. We plot the evolution of $H(z)/1+z$ in Figure 5. Our results in Tables 1 and Figure 6 show that the assumption of dependence dark matter to k scale can only reduce the S_8 tension and not the H_0 tension. In general, k -DM(1) model, which considered the equation of state, w , and adiabatic sound speed, c_g^2 independent of k scale, reduces S_8 tension more than other models.

³ The only Planck-constrained parameters are not shown in the figures, but it has checked that Planck and Planck+Other are consistent. This means the contours for the latter are inside the only Planck contours.

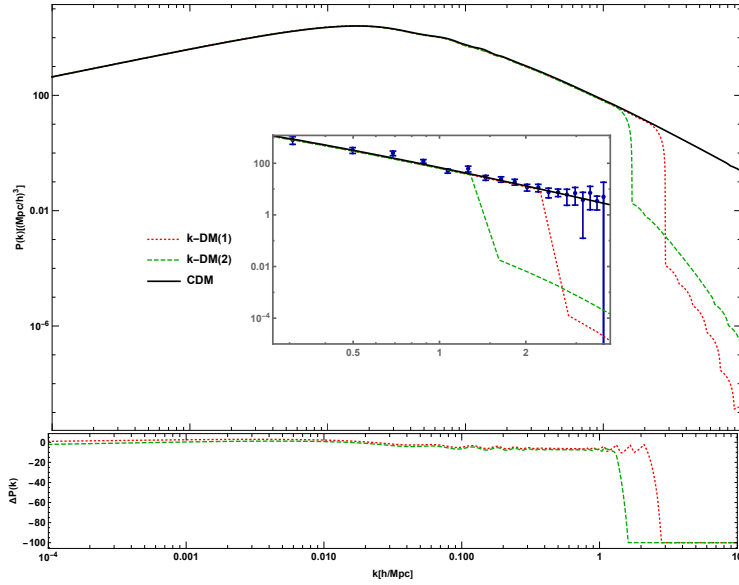


Figure 2. The matter power spectrum for k -Dependent DM and CDM models, and the fractional difference between them. The behavior of k -DM models mimics the CDM for small k 's. However, we see a transition for large k 's in k -DM models. However, there is no very precise data points at those scales.

Table 2. The result of MCMC analysis for the best-fit χ^2 , and AIC. It shows that k -DM models have more space to have Planck+Other datasets altogether consistently.

Parameters	CDM		k-DM(1)		k-DM(2)	
	<i>Planck</i>	<i>Planck + Other</i>	<i>Planck</i>	<i>Planck + Other</i>	<i>Planck</i>	<i>Planck + Other</i>
χ^2_{\min}	2780.9	3824	2781.02	3812.2	2780.44	3816.7
$\text{AIC}_{k\text{-DM}(i)} - \text{AIC}_{\text{CDM}}$	0	0	8.12	-3.8	5.54	-1.3

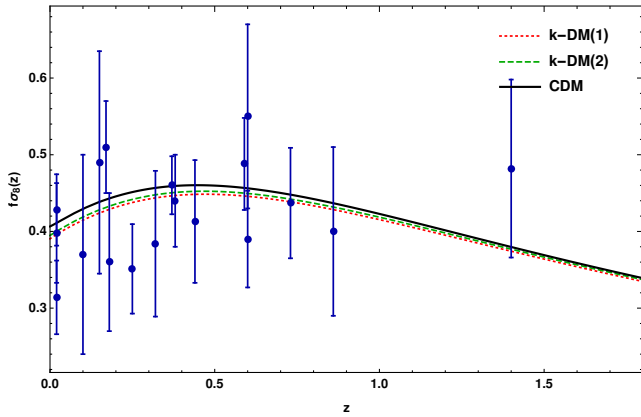


Figure 3. The growth rate of matter fluctuations for k -Dependent DM model compared to CDM model. The observational constraints are taken from (Kazantzidis & Perivolaropoulos 2018).

4 DISCUSSION

The warm dark matter model has always been of interest mainly because of the possible need to alleviate the small-scale problems of the Λ CDM. With such insight and also motivated by the effect of adding this cosmological compo-

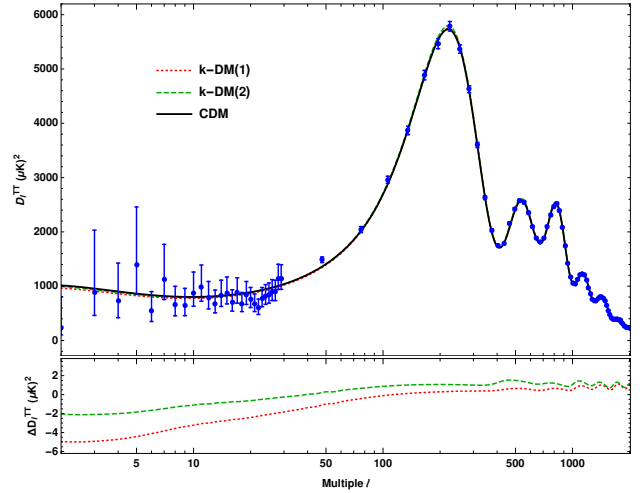


Figure 4. Temperature anisotropies in the CMB. The bottom part of the panel displays the relative temperature differences between the k -DM and the CDM model.

ment to reduce current cosmological tensions, in this work we considered a scenario in which the behavior of dark matter depends on the scale. It mimics CDM for small k 's and

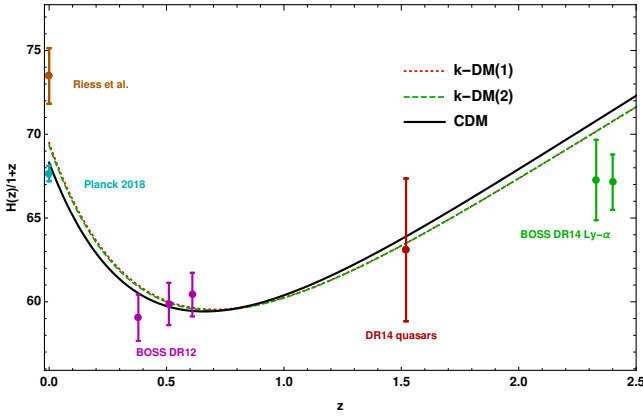


Figure 5. The redshift evolution of $H(z)/1+z$ using the best fit values of cosmological parameters in Tables 1 by Planck+Other data for the proposed k -DM scenarios and CDM model. Also, in the Figure, the observational data points from the Riess et al. (Riess et al. 2019), Planck 2018 (Aghanim et al. 2020), BOSS DR12 (Alam et al. 2017), DR14 quasars (Zarrouk et al. 2018), and BOSS DR14 Ly- α (de Sainte Agathe et al. 2019) measurements have been specified for comparison.

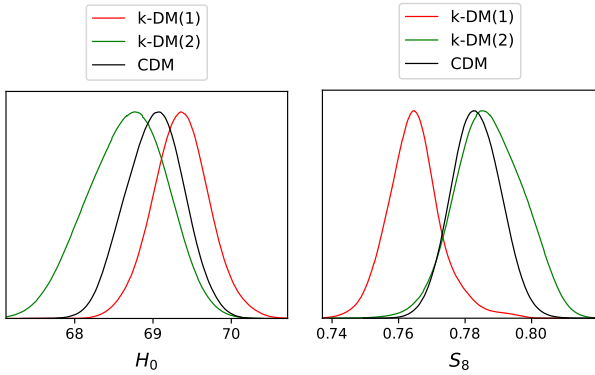


Figure 6. Comparison between H_0 and S_8 tensions for all considered models in this study using the Planck+Other data.

WDM for large k 's. A motivation for us was to check if the trace of WDM, which can be seen in very small scales to address e.g., can the core-cusp problem show itself in the (very short) cosmological scales? Our results show that this transition can affect the amplitude of the matter fluctuations, such that reducing the S_8 tension. However, it seems the lack of cosmological data for very large k 's makes it hard to answer to the above question. For future analysis, we can think of a more theoretical framework and also find cosmological datas at very small scales which are cleaned from the baryonic physics. One way can be tracing the effects of our model in non-linear structure formation and the dark matter halo distributions.

5 ACKNOWLEDGMENTS

NK would like to thank Marzieh Farhang for instructive discussions during working on Farhang & Khosravi (2023). This

work has been supported financially by a grant from Basic Sciences Research Fund under grant number BSRF-phys-399-06. ZD also acknowledges support from Iran Science Elites Federation under grant number M401543.

6 DATA AVAILABILITY

No new data were generated or analysed in support of this research.

References

Abellán G. F., Murgia R., Poulin V., 2021, *Phys. Rev. D*, 104, 123533

Ade P. A. R., et al., 2016, *Astron. Astrophys.*, 594, A24

Aghanim N., et al., 2020, *Astron. Astrophys.*, 641, A6

Alam S., et al., 2017, *Mon. Not. Roy. Astron. Soc.*, 470, 2617

Aoyama S., Sekiguchi T., Ichiki K., Sugiyama N., 2014, *JCAP*, 07, 021

Archidiacono M., Hooper D. C., Murgia R., Bohr S., Lesgourgues J., Viel M., 2019, *JCAP*, 10, 055

Audren B., Lesgourgues J., Benabed K., Prunet S., 2013, *JCAP*, 02, 001

Blomqvist M., et al., 2019, *Astron. Astrophys.*, 629, A86

Brinckmann T., Lesgourgues J., 2019, *Phys. Dark Univ.*, 24, 100260

Buen-Abad M. A., Emami R., Schmaltz M., 2018, *Phys. Rev. D*, 98, 083517

Davari Z., Khosravi N., 2022, *Mon. Not. Roy. Astron. Soc.*, 516, 4373

Davari Z., Rahvar S., 2021, *Mon. Not. Roy. Astron. Soc.*, 507, 3387

Davari Z., Malekjani M., Artymowski M., 2018, *Phys. Rev. D*, 97, 123525

Diamanti R., Ando S., Gariazzo S., Mena O., Weniger C., 2017, *JCAP*, 06, 008

Farhang M., Khosravi N., 2021, *Phys. Rev. D*, 103, 083523

Farhang M., Khosravi N., 2023

Gelman A., Rubin D. B., 1992, *Statist. Sci.*, 7, 457

Gentile G., Salucci P., Klein U., Vergani D., Kalberla P., 2004, *Mon. Not. Roy. Astron. Soc.*, 351, 903

Gilman D., Birrer S., Nierenberg A., Treu T., Du X., Benson A., 2020, *Mon. Not. Roy. Astron. Soc.*, 491, 6077

Hildebrandt H., et al., 2020, *Astron. Astrophys.*, 633, A69

Hsueh J.-W., Enzi W., Vegetti S., Auger M., Fassnacht C. D., Despali G., Koopmans L. V. E., McKean J. P., 2020, *Mon. Not. Roy. Astron. Soc.*, 492, 3047

Ilić S., Kopp M., Skordis C., Thomas D. B., 2021, *Phys. Rev. D*, 104, 043520

Kazantzidis L., Perivolaropoulos L., 2018, *Phys. Rev. D*, 97, 103503

Kazin E. A., et al., 2014, *Mon. Not. Roy. Astron. Soc.*, 441, 3524

Khosravi N., Farhang M., 2022, *Phys. Rev. D*, 105, 063505

Kopp M., Skordis C., Thomas D. B., 2016, *Phys. Rev. D*, 94, 043512

Lesgourgues J., Tram T., 2011, *JCAP*, 09, 032

Loeb A., Weiner N., 2011, *Phys. Rev. Lett.*, 106, 171302

Maccio A. V., Ruchayskiy O., Boyarsky A., Munoz-Cuartas J. C., 2013, *Mon. Not. Roy. Astron. Soc.*, 428, 882

Menci N., Sanchez N. G., Castellano M., Grazian A., 2016, *Astrophys. J.*, 818, 90

Moore B., Ghigna S., Governato F., Lake G., Quinn T. R., Stadel J., Tozzi P., 1999, *Astrophys. J. Lett.*, 524, L19

Pacucci F., Mesinger A., Haiman Z., 2013, *Mon. Not. Roy. Astron. Soc.*, 435, L53

Paribelli G., Scelfo G., Giri S. K., Schneider A., Archidiacono M., Camera S., Viel M., 2021, *JCAP*, 12, 044

- Purcell C. W., Zentner A. R., 2012, *JCAP*, 12, 007
- Riess A. G., Casertano S., Yuan W., Macri L. M., Scolnic D., 2019, *Astrophys. J.*, 876, 85
- Rubin V. C., Ford Jr. W. K., 1970, *Astrophys. J.*, 159, 379
- Rubin V. C., Thonnard N., Ford Jr. W. K., 1980, *Astrophys. J.*, 238, 471
- Scolnic D. M., et al., 2018, *Astrophys. J.*, 859, 101
- Scott D., 2020, *Proc. Int. Sch. Phys. Fermi*, 200, 133
- Tram T., Brandbyge J., Dakin J., Hannestad S., 2019, *JCAP*, 03, 022
- Zarrouk P., et al., 2018, *Mon. Not. Roy. Astron. Soc.*, 477, 1639
- Zu L., Zhang C., Chen H.-Z., Wang W., Tsai Y.-L. S., Tsai Y., Luo W., Fan Y.-Z., 2023
- de Sainte Agathe V., et al., 2019, *Astron. Astrophys.*, 629, A85
- de Souza R. S., Mesinger A., Ferrara A., Haiman Z., Perna R., Yoshida N., 2013, *Mon. Not. Roy. Astron. Soc.*, 432, 3218